Synthesis, characterization and thermal properties of nine quaternary dialkyldiaralkylammonium chlorides

Sara Busi, Manu Lahtinen *, Minna Kärnä, Jussi Valkonen,
Erkki Kolehmainen, Kari Rissanen

Department of Chemistry, University of Jyväskylä, P.O. Box 35, FIN-40014 Jyväskylä, Finland

Abstract

Nine $R_2R_2'N^+Cl^-$ (R=benzyl, 2-methylbenzyl, 3-methylbenzyl, 4-methylbenzyl, 2-phenylethyl or 3-phenylpropyl; R'=ethyl or methyl) quaternary dialkyldiaralkylammonium chlorides were synthesized by treating dimethylformamide or diethylformamide with non-substituted or substituted arylalkyl (aralkyl) halide in the presence of sodium carbonate. The ^1H NMR, ^{13}C NMR spectroscopy, mass spectroscopy and elemental analysis were used to characterize the synthesized products. The crystal structures of six compounds were determined by X-ray single crystal diffraction. Four of the compounds crystallized in monoclinic space groups $C2/c$ and $P2_1/c$ (or $P2_1/n$), one in triclinic space group $P-1$ and one in orthorhombic space group Pbca. The powder diffraction method was used to compare the structural similarities between the single crystal and the microcrystalline bulk composition. Thermal properties of the new compounds were studied using TG/DTA and DSC methods. The decomposition of the compounds started generally between 130–185 °C and occurred without identifiable cleavages. The synthesized compounds do not seem to be suitable for ionic liquid applications because no melting point was observed for most of them. However, the good thermal stability of these compounds enables their potential use for example as phase-transfer catalysts and electrolytes.
© 2005 Elsevier B.V. All rights reserved.

Keywords: Quaternary dialkyldiaralkylammonium chloride; X-ray single crystal diffraction; X-ray powder diffraction; Thermal analysis

1. Introduction

Quaternary ammonium halides have been used as catalysts, electrolytes and surfactants in various applications [1–11]. Indeed, the presence of dihexyldimethylammonium chloride in the detergent mixture provides good detergency in the washing of textiles containing oily and greasy soils [12]. Furthermore, quaternary ammonium chlorides have been utilized in electrochemical synthesis of layered manganese oxides [13] and have been also used in the electrolyte solutions of primary and secondary alkaline zinc batteries [14]. The small alkyl ammonium cations have shown to be useful guest candidates for resorcinarene complexation as the alkyl ammonium cations can interact via cation⋯π and C–H⋯π interactions as well as fill the hollow cavity of the electron-rich resorcinarene host [15–20]. In addition to resorcinarenes, considerable numbers of other complexes have also been examined, such as the tetraalkylammonium halides with carbon tetrahalides and with tetrahaloethylenes [21]. The copper(II) chloride complexes have been a subject of interest because of their structural properties, phase transitions and thermochromic behavior in the solid state [22–28].

The quaternary arylalkyl (aralkyl) ammonium cations are not as well-known as the quaternary alkyl ammonium cations. The recently reported one-pot synthesis has enabled the production of pure $R_2R_2'N^+X^-$ type quaternary ammonium halides, in which R represents the alkyl or the aralkyl group [29–31]. In this study, nine $R_2R_2'N^+X^-$ type quaternary dialkyldiaralkylammonium chlorides have been synthesized and characterized. Two of the compounds, dibenzyldimethylammonium chloride and diethyldibenzylammonium chloride, are known and their usability in various applications has been studied earlier by other groups but the detailed characterization of the compounds themselves has not been the main focus of these studies [32–41]. Herein the thorough characterization of nine aromatic quaternary dialkyldiaralkylammonium chlorides is reported. Dimethyldi(4-methylbenzyl) ammonium chloride has been briefly presented in a previous publication when the new synthetic route was introduced [29]. In this paper, ^1H and ^{13}C NMR spectroscopy, ESI-TOF MS measurements and elemental analysis are used for

---

* Corresponding author. Tel.: +358 14 2602624; fax: +358 14 2602501.
E-mail address: makrla@cc.jyu.fi (M. Lahtinen).

the characterization of the compounds. Six new crystal structures have been determined by X-ray single crystal diffraction. The powder diffraction analyses were measured to confirm the structural similarities between the single crystal structure and the microcrystalline bulk composition. The thermal properties have been observed by TG/DTA and DSC methods. The synthesized quaternary dialkyldiaralkylammonium chlorides proved to be thermally stable because two of the compounds have relatively high melting points and six of the compounds showed no melting point up to their decomposition (starting at 130–185 °C), therefore promoting their use, for example, as phase-transfer catalysts and electrolytes.

The main aim of our study is to broaden the existence range of the $R_2R'_2N^+X^-$ type quaternary ammonium compounds. In addition, the applicability of the above-mentioned quaternary ammonium chlorides for ionic liquid applications is to be enhanced in the near future by using an anion exchange method. With the combination of proper cation and anion pairs, the physical and chemical properties of the compounds can be extensively altered. In addition, the synthesis of the $(R_2R'_2N^+X^-)_2$ MCl_4 (M = Mn, Fe, Co, Ni, Cu, Zn) series of compounds will be the focus of further studies as the A_2MX_4 structures and their phase behavior have been of considerable interest to solid state scientists for some time [22–28]. With new $R_2R'_2N^+X^-$ type quaternary dialkyldiaralkylammonium halides the effects of the aralkyl groups on the structures and the phase behavior of the $(R_2R'_2N^+X^-)_2MCl_4$ compounds can be examined.

2. Experimental section

2.1. Synthesis and analysis

2.1.1. General procedure

Compounds **1**–**9** (Scheme 1) were synthesized by using a one-pot synthesis route described earlier [29]. All reagents and solvents were used as received from the manufacturers. Suitable quantities of formamide and aralkylchloride were placed together within a reaction flask in the presence of sodium carbonate and the reaction mixture was stirred at 80–100 °C for 72–96 h. After cooling down to RT the mixture was filtered and the filtrate was evaporated. The extraction of the product was performed with one of the two following methods.

Method A. A small amount of acetone, diethyl ether or their mixture was added to the residue to give a white or light yellow powder. The powder was washed with diethyl ether and dried in vacuo overnight.

Method B. The residue (from evaporation of the filtrate) was dissolved in a water/diethyl ether solution. The water layer was separated and evaporated resulting in the product as a pure gel. The gel was washed with dichloromethane and dried *in vacuo*.

2.1.2. Dibenzyldimethylammonium chloride (**1**)

Method A. Reagents: benzyl chloride (8.79 ml, 76.40 mmol), sodium carbonate (8.10 g, 76.40 mmol) and dimethyl formamide (30 ml). Reaction temperature 80 °C and reaction time 72 h. The yield (white powder) was 4.87 g (49%). ^{1}H NMR (CDCl$_3$, 500 MHz, ppm): 3.14 (6H, s, N–C**H**$_3$), 5.18 (4H, s, Ph–C**H**$_2$), 7.36 (4H, t, Ar–**H**(3,5)), 7.42 (2H, t, Ar–**H**(4)), 7.67 (4H, d, Ar–**H**(2,6)). ^{13}C NMR (CDCl$_3$, 126 MHz, ppm): 48.09 (2C, N–**C**H$_3$), 67.63 (2C, Ph–**C**H$_2$), 127.64 (2C, Ar–**C**(1)), 129.06 (4C, Ar–**C**(3,5)), 130.52 (2C, Ar–**C**(4)), 133.42 (4C, Ar–**C**(2,6)). ESI-TOF MS: *m/z* calculated for C$_{16}$H$_{20}$NCl [M−Cl]$^+$: 226.16; found: 226.06 [M−Cl]$^+$. Elemental Analysis: Calculated for C$_{16}$H$_{20}$NCl: C, 73.41; H, 7.70; N, 5.35. Found: C, 73.17; H, 7.69; N, 5.01.

2.1.3. Dimethyldi(2-methylbenzyl)ammonium chloride (**2**)

Method A. Reagents: 2-methylbenzyl chloride (9.13 ml, 69.00 mmol), sodium carbonate (7.31 g, 69.00 mmol) and dimethyl formamide (50 ml). Reaction temperature 80 °C and
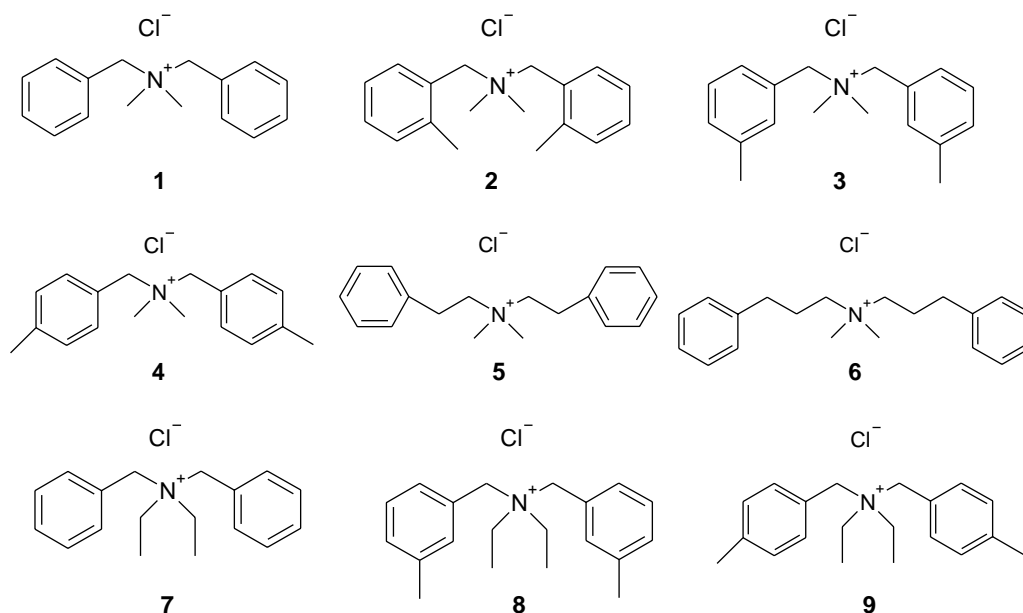
Scheme 1. Molecular structures of the compounds **1**–**9**.

reaction time 72 h. The yield (white powder) was 2.30 g (23%). ^{1}H NMR (CDCl$_3$, 500 MHz, ppm): 2.50 (6H, s, C**H**$_3$), 3.14 (6H, s, C**H**$_3$), 5.26 (4H, s, Ph–C**H**$_2$), 7.22 (2H, t, Ar–**H**), 7.25 (2H, d, Ar–**H**), 7.33 (2H, td, Ar–**H**), 7.69 (2H, dd, Ar–**H**). ^{13}C NMR (CDCl$_3$, 126 MHz, ppm): 20.64 (2C, C**H**$_3$), 48.29 (2C, C**H**$_3$), 65.20 (2C, Ph–C**H**$_2$), 126.08 (2C, Ar–**C**), 126.46 (2C, Ar–**C**), 130.71 (2C, Ar–**C**), 131.83 (2C, Ar–**C**), 135.15 (2C, Ar–**C**), 140.12 (2C, Ar–**C**). ESI-TOF MS: *m/z* calculated for C$_{18}$H$_{24}$NCl [M−Cl]$^+$: 254.19; found: 254.12 [M−Cl]$^+$. Elemental Analysis: Calculated for C$_{18}$H$_{24}$NCl: C, 74.59; H, 8.35; N, 4.83. Found: C, 73.74; H, 8.34; N, 4.54.

2.1.4. Dimethyldi(3-methylbenzyl)ammonium chloride (3)

Method A. Reagents: 3-methylbenzyl chloride (9.12 ml, 69.00 mmol), sodium carbonate (7.31 g, 69.00 mmol) and dimethyl formamide (50 ml). Reaction temperature 75 °C and reaction time 72 h. The yield (white powder) was 3.5 g (35%). ^{1}H NMR (CDCl$_3$, 500 MHz, ppm): 2.23 (6H, s, C**H**$_3$), 3.11 (6H, s, C**H**$_3$), 5.08 (4H, s, Ph–C**H**$_2$), 7.17 (2H, d, Ar–**H**), 7.20 (2H, t, Ar–**H**), 7.39 (2H, s, Ar–**H**(2)), 7.43 (2H, d, Ar–**H**). ^{13}C NMR (CDCl$_3$, 126 MHz, ppm): 21.10 (2C, C**H**$_3$), 48.08 (2C, C**H**$_3$), 67.58 (2C, Ph–C**H**$_2$), 127.50 (2C, Ar–**C**(1)), 128.78 (2C, Ar–**C**), 130.47 (2C, Ar–**C**), 131.15 (2C, Ar–**C**), 133.72 (2C, Ar–**C**(2)), 138.80 (2C, Ar–**C**). ESI-TOF MS: *m/z* calculated for C$_{18}$H$_{24}$NCl [M−Cl]$^+$: 254.19; found: 254.07 [M−Cl]$^+$. Elemental analysis: calculated for C$_{18}$H$_{24}$NCl: C, 74.59; H, 8.35; N, 4.83. Found: C, 74.26; H, 8.36; N, 4.60.

2.1.5. Dimethyldi(4-methylbenzyl)ammonium chloride (4)

Method A. Reagents: 4-methylbenzyl chloride (9.15 ml, 69.00 mmol), sodium carbonate (7.31 g, 69.00 mmol) and dimethyl formamide (30 ml). Reaction temperature 80 °C and reaction time 72 h. The yield (white powder) was 6.82 g (68%). ^{1}H NMR (CDCl$_3$, 500 MHz, ppm): 2.32 (6H, s, C**H**$_3$), 3.08 (6H, s, C**H**$_3$), 5.05 (4H, s, Ph–C**H**$_2$), 7.14 (4H, d, Ar–**H**), 7.51 (4H, d, Ar–**H**). ^{13}C NMR (CDCl$_3$, 126 MHz, ppm): 21.21 (2C, C**H**$_3$), 47.93 (2C, C**H**$_3$), 67.44 (2C, Ph–C**H**$_2$), 124.54 (2C, Ar–**C**), 129.70 (4C, Ar–**C**), 133.25 (4C, Ar–**C**), 140.69 (2C, Ar–**C**). ESI-TOF MS: *m/z* calculated for C$_{18}$H$_{24}$NCl [M−Cl]$^+$: 254.19; found: 254.04 [M−Cl]$^+$. Elemental analysis: calculated for C$_{18}$H$_{24}$NCl: C, 74.59; H, 8.35; N, 4.83. Found: C, 74.39; H, 8.41; N, 4.59.

2.1.6. Dimethyldi(2-phenylethyl)ammonium chloride (5)

Method A. Reagents: 2-phenylethyl chloride (9.08 ml, 69.00 mmol), sodium carbonate (7.31 g, 69.00 mmol) and dimethyl formamide (30 ml). Reaction temperature 90 °C and reaction time 72 h. The yield (light yellow powder) was 0.17 g (2%). ^{1}H NMR (CDCl$_3$, 500 MHz, ppm): 3.06–3.09 (4H, m, N–C**H**$_2$CH$_2$–Ph), 3.50 (6H, s, N–C**H**$_3$), 3.88–3.91 (4H, m, N–CH$_2$C**H**$_2$–Ph), 7.23–7.26 (2H, m, Ar–**H**(4)), 7.28–7.32 (8H, m, Ar–**H**). ^{13}C NMR (CDCl$_3$, 126 MHz, ppm): 29.42 (2C, N–CH$_2$**C**H$_2$–Ph), 51.34 (2C, N–**C**H$_3$), 64.58 (2C, N–**C**H$_2$CH$_2$–Ph), 127.56 (2C, Ar–**C**(4)), 129.02 (4C, Ar–**C**), 129.15 (4C, Ar–**C**), 134.72 (2C, Ar–**C**(1)). ESI-TOF MS: *m/z* calculated for C$_{18}$H$_{24}$NCl [M−Cl]$^+$: 254.19; found: 254.07 [M−Cl]$^+$.

Elemental analysis: calculated for C$_{18}$H$_{24}$NCl: C, 74.59; H, 8.35; N, 4.83. Found: C, 73.16; H, 8.28; N, 4.59.

2.1.7. Dimethyldi(3-phenylpropyl)ammonium chloride (6)

Method B. Reagents: 3-phenylpropyl chloride (9.30 ml, 62.91 mmol), sodium carbonate (6.67 g, 62.91 mmol) and dimethyl formamide (30 ml). Reaction temperature 100 °C and reaction time 72 h. The yield (brown gel) was 1.4 g (14%) . ^{1}H NMR (CDCl$_3$, 500 MHz, ppm): 1.86–1.93 (4H, m, N–C**H**$_2$CH$_2$CH$_2$–Ph), 2.67 (4H, t, N–CH$_2$CH$_2$C**H**$_2$–Ph), 3.36 (6H, s, N–C**H**$_3$), 3.47–3.50 (4H, m, N–C**H**$_2$CH$_2$CH$_2$–Ph), 7.11–7.14 (4H, m, Ar–**H**(2,6)), 7.18–7.21 (2H, m, Ar–**H**(4)), 7.25–7.29 (4H, m, Ar–**H**(3,5)). ^{13}C NMR (CDCl$_3$, 126 MHz, ppm): 24.30 (2C, N–CH$_2$**C**H$_2$CH$_2$–Ph), 31.98 (2C, N–CH$_2$CH$_2$**C**H$_2$–Ph), 51.45 (2C, N–**C**H$_3$), 62.73 (2C, N–**C**H$_2$CH$_2$CH$_2$–Ph), 126.76 (2C, Ar–**C**(4)), 128.32 (4C, Ar–**C**(2,6)), 128.79 (4C, Ar–**C**(3,5)), 139.25 (2C, Ar–**C**(1)). ESI-TOF MS: *m/z* calculated for C$_{20}$H$_{28}$NCl [M−Cl]$^+$: 282.22; found: 282.08 [M−Cl]$^+$. Elemental analysis: calculated for C$_{20}$H$_{28}$NCl: C, 75.56; H, 8.88; N, 4.41. Found: C, 73.77; H, 9.18; N, 4.52.

2.1.8. Dibenzyldiethylammonium chloride (7)

Method A. Reagents: benzyl chloride (7.94 ml, 69.00 mmol), sodium carbonate (7.31 g, 69.00 mmol) and diethyl formamide (50 ml). Reaction temperature 60 °C and reaction time 72 h. The yield (light brown powder) was 0.40 g (4%). ^{1}H NMR (CDCl$_3$, 500 MHz, ppm): 1.37 (6H, t, N–CH$_2$C**H**$_3$), 3.58 (4H, q, N–C**H**$_2$CH$_3$), 5.05 (4H, s, Ph–C**H**$_2$), 7.40–7.46 (6H, m, Ar–**H**), 7.66–7.68 (4H, m, Ar–**H**). ^{13}C NMR (CDCl$_3$, 126 MHz, ppm): 9.50 (2C, N–CH$_2$**C**H$_3$), 52.91 (2C, N–**C**H$_2$CH$_3$), 64.10 (2C, Ph–C**H**$_2$), 127.94 (2C, Ar–**C**(1)), 129.31 (4C, Ar–**C**), 130.60 (2C, Ar–**C**(4)), 133.07 (4C, Ar–**C**). ESI-TOF MS: *m/z* calculated for C$_{18}$H$_{24}$NCl [M−Cl]$^+$: 254.19; found: 254.07 [M−Cl]$^+$. Elemental analysis: calculated for C$_{18}$H$_{24}$NCl: C, 74.59; H, 8.35; N, 4.83. Found: C, 73.93; H, 8.40; N, 4.65.

2.1.9. Diethyldi(3-methylbenzyl)ammonium chloride (8)

Method B. Reagents: 3-methylbenzyl chloride (8.70 ml, 65.82 mmol), sodium carbonate (6.98 g, 65.82 mmol) and diethyl formamide (50 ml). Reaction temperature 80 °C and reaction time 96 h. The yield (light yellow sticky powder) was 0.60 g (6%). ^{1}H NMR (CDCl$_3$, 500 MHz, ppm): 1.35 (6H, t, N–CH$_2$C**H**$_3$), 2.30 (6H, s, Ph–C**H**$_3$), 3.48 (4H, q, N–C**H**$_2$CH$_3$), 4.87 (4H, s, Ph–C**H**$_2$), 7.19–7.25 (4H, m, Ar–**H**), 7.36–7.38 (4H, m, Ar–**H**). ^{13}C NMR (CDCl$_3$, 126 MHz, ppm): 9.38 (2C, N–CH$_2$**C**H$_3$), 21.20 (2C, Ph–**C**H$_3$), 52.86 (2C, N–**C**H$_2$CH$_3$), 63.78 (2C, Ph–**C**H$_2$), 127.67 (2C, Ar–**C**), 129.00 (2C, Ar–**C**), 129.93 (2C, Ar–**C**), 131.19 (2C, Ar–**C**), 133.40 (2C, Ar–**C**), 139.03 (2C, Ar–**C**). ESI-TOF MS: *m/z* calculated for C$_{20}$H$_{28}$NCl [M−Cl]$^+$: 282.22; found: 282.08 [M−Cl]$^+$. Elemental Analysis: Calculated for C$_{20}$H$_{28}$NCl: C, 75.56; H, 8.88; N, 4.41. Found: C, 69.58; H, 8.52; N, 4.34.

2.1.10. Diethyldi(4-methylbenzyl)ammonium chloride (9)

Method B. Reagents: 4-methylbenzyl chloride (8.73 ml, 65.82 mmol), sodium carbonate (6.98 g, 65.82 mmol) and diethyl formamide (50 ml). Reaction temperature 80 °C and reaction time 96 h. The yield (light yellow sticky powder) was 0.97 g (10%). ^1H NMR (CDCl$_3$, 500 MHz, ppm): 1.35 (6H, t, N–CH$_2$CH$_3$), 2.32 (6H, s, Ph–CH$_3$), 3.46 (4H, q, N–CH$_2$CH$_3$), 4.88 (4H, s, N–CH$_2$–Ph), 7.16 (4H, d, Ar–H), 7.47 (4H, d, Ar–H). ^{13}C NMR (CDCl$_3$, 126 MHz, ppm): 9.40 (2C, N–CH$_2$CH$_3$), 21.17 (2C, Ph–CH$_3$), 52.66 (2C, N–CH$_2$CH$_3$), 63.45 (2C, N–CH$_2$–Ph), 124.74 (2C, Ar–C), 129.85 (4C, Ar–C), 132.79 (4C, Ar–C), 140.69 (2C, Ar–C). ESI-TOF MS: m/z calculated for C$_{20}$H$_{28}$NCl [M−Cl]$^+$: 282.22; found: 282.08 [M−Cl]$^+$. Elemental analysis: calculated for C$_{20}$H$_{28}$NCl: C, 75.56; H, 8.88; N, 4.41. Found: C, 70.87; H, 8.70; N, 4.40.

2.2. Characterization in the liquid state

^1H and ^{13}C NMR spectroscopy and ESI TOF MS methods were used to confirm the formation of quaternary dialkyldiaralkylammonium halides. The purity of synthesized compounds was verified with elemental analysis. ^1H NMR spectra and ^{13}C NMR spectra were measured in CDCl$_3$ at 30 °C by using a Bruker Avance DRX 500 NMR spectrometer operating at 500 MHz for ^1H and 126 MHz for ^{13}C. Electrospray mass spectrometric measurements were obtained by using the Micromass LCT time of flight (TOF) mass spectrometer with electrospray ionization (ESI). The compounds were measured by using the positive ion mode with a sample concentration of 25 mg/l in a methanol solution. The elemental analyses were carried out with Vario EL III CHN elemental analyzer by using sample weights of 3–5 mg.
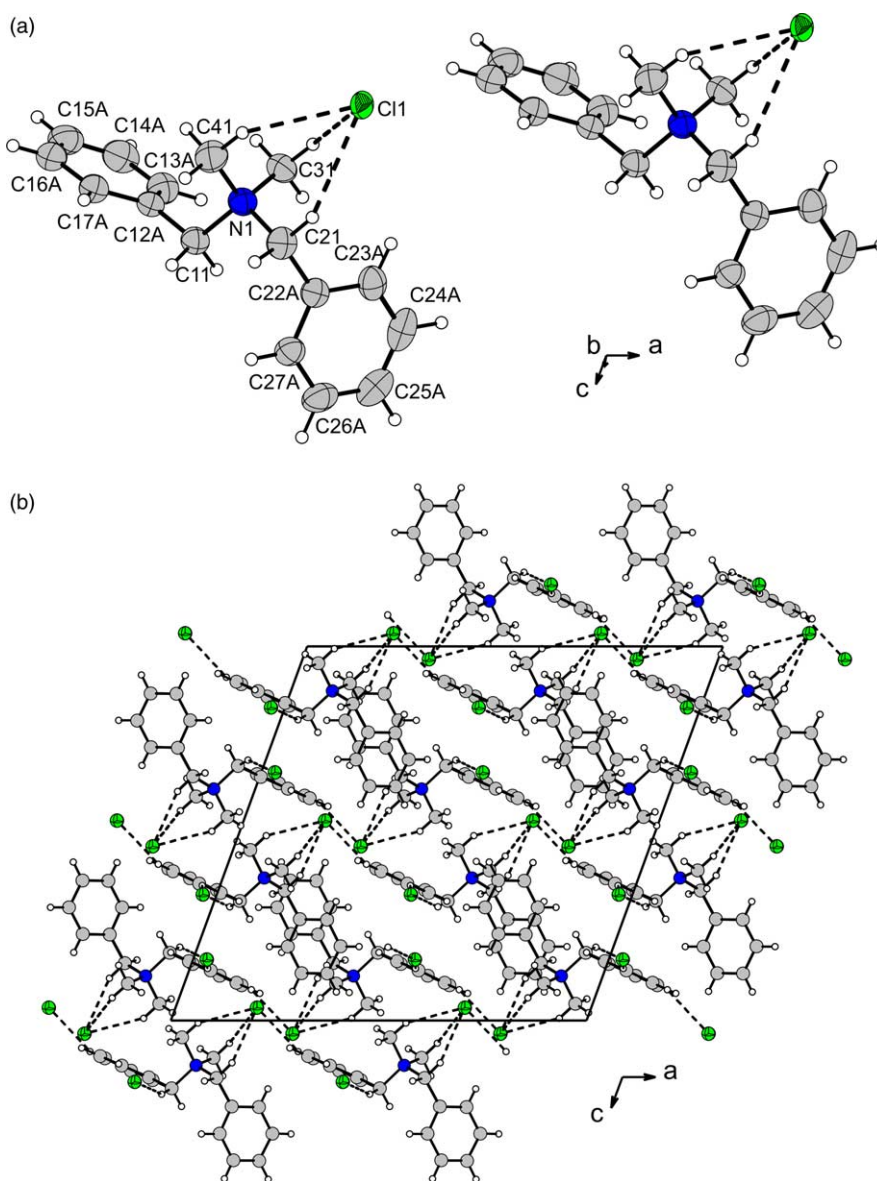

Fig. 1. (a) The ion-pair ordering of compound **1** with numbering scheme (thermal ellipsoids are presented at 50% probability level in all figures). The other disordered chloride atom is omitted for clarity. (b) Packing of **1** along the crystallographic *b*-axis with hydrogen bonding (Cl$^-$···H–C < 2.8 Å) shown as dashed lines. The shortest cation/anion distances are C15A···Cl1 3.55(4) Å and C41···Cl1 3.61(2) Å. The distance of the chloride anion to the nearest nitrogen (Cl$^-$···N$^+$) atom is about 3.85(2) Å.
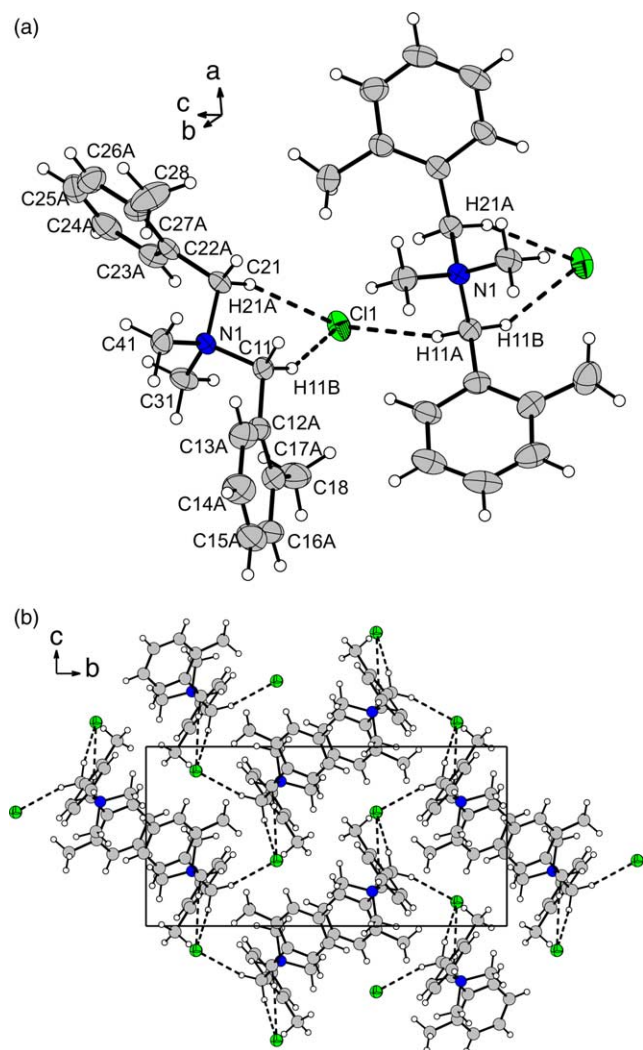
Fig. 2. (a) The ion-pair ordering of compound **2**. (b) Crystal packing with hydrogen bonding (Cl$^-$···H–C < 2.8 Å) shown as dashed lines viewed from along the crystallographic *a*-axis. The shortest cation/anion distances are C21···Cl1 3.56(1) and C11···Cl1 3.59(1). The distance from chloride anion to the adjacent nitrogen atoms is 3.97(1) Å.

2.3. X-ray single crystal structures

The X-ray structures for compounds **1–5** and **7** were determined by X-ray single crystal diffraction. Colorless single crystals of compounds **1–5** and **7** were recrystallized from a MeOH/EtOAc solution. Compounds **8** and **9** remained as sticky powders and compound **6** as a viscous gel, despite numerous attempts to solidify them. Single crystals of compounds **6**, **8** and **9**, therefore, could not be obtained.

The crystallographic data were recorded with a Nonius KappaCCD diffractometer at −100 °C using graphite monochromatized MoK$_\alpha$ ($\lambda = 0.71069$ Å) radiation. The data were processed with EvalCCD [42] software package and the absorption correction was performed using SADABS (included in EvalCCD software package). All the structures were solved with direct methods (SIR92 [43], SIR97 [44]) and refined on F^2 by full-matrix least-squares techniques (SHELXL-97 [45]) by using anisotropic temperature factors

for all non-H atoms. All the hydrogen atoms were calculated for their ideal positions as riding atoms by using isotropic temperature factors.

2.4. X-ray powder diffraction analyses

X-ray powder diffraction measurements of compounds **1–5** and **7** were carried out at room temperature with a Huber imaging-plate Guinier diffractometer 670. The sealed-tube X-ray generator system was operated at 45 kV and 25 mA and pure line-focused CuKα_1 radiation ($\lambda = 1.5406$ Å) was produced by primary beam curved germanium monochromator. The samples were measured in a Guinier-type transmission geometry with the angle of incidence 45° to the sample normal. The X-ray diffraction data were recorded
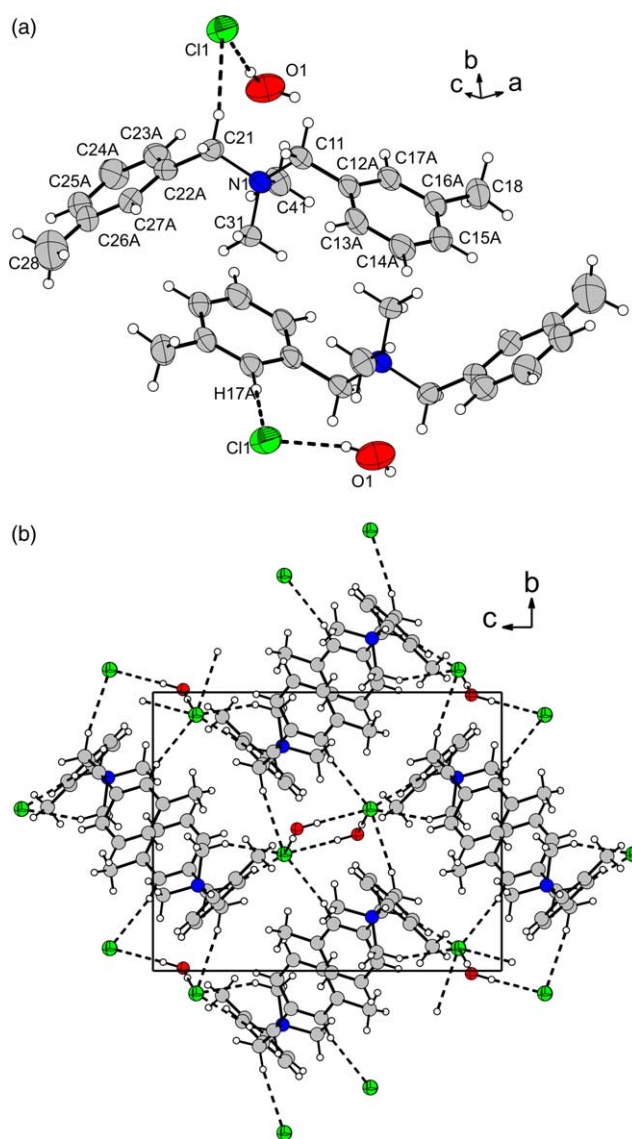

Fig. 3. (a) The ion-pair ordering of compound **3**. (b) The packing mode of **3**. The hydrogen bonds (Cl$^-$···H–C < 2.8 Å) are shown as dashed lines. The hydrogen bond distances are Cl1···H1A–O1 2.29(4) Å and Cl1···H1B–O1 2.30(3) Å. The shortest cation/anion distances are C11···Cl1 3.53(1) Å and C31···Cl1 3.58(1) Å. The distance from chloride anion to the adjacent nitrogen atom is 3.86(1) Å.

using the curved imaging plate in the 2θ angle range from 4 to 100° with recording time of 20 min and resolution step of 0.005°.

2.5. Solid state NMR

^{13}C CP/MAS NMR spectra were measured to work out the morphology of the compounds **1** and **3**. The spectra were measured with a Bruker Avance 400 spectrometer equipped with 4 mm standard bore CP/MAS probe-head using 4 mm diameter zirconia rotor and Kel-F caps at ambient temperature. The samples were spun at 15 KHz speed because at lower speeds the spinning side bands were clearly visible. The contact time was 2 ms.

2.6. Thermal properties

The thermal decomposition paths of compounds **1–9** were obtained with PerkinElmer Diamond TG/DTA. Measurements were carried out using platinum pans under synthetic air atmosphere (flow rate of 135 ml/min) at a temperature range of 25–600 °C (heating rate of 10 °C/min). The temperature calibration of the TG/DTA equipment was carried out using melting points of five reference materials (In, Sn, Zn, Al, Au). The weight balance was calibrated by measuring the standard weight as function of temperature. The sample weights used in the measurements were about 5–20 mg.

The thermal behavior of the compounds was examined with a Perkin–Elmer PYRIS 1 DSC. The observed melting points were also confirmed with a Mettler Toledo FP62 melting point instrument (not corrected) to help the interpretation of DSC curves. DSC measurements were carried out (under nitrogen atmosphere 50 ml/min) using 50 μl sealed aluminum sample pans with pinholes. The temperature calibration was made using three standard materials (n-decane, In, Zn) and the energy calibration by indium standard. The samples were heated at a rate of 10 °C/min from −50 °C up to the temperature close to the predetermined (DSC, TG/DTA) decomposition temperature of each compound. The sample weights used in the measurements were about 3–6 mg.
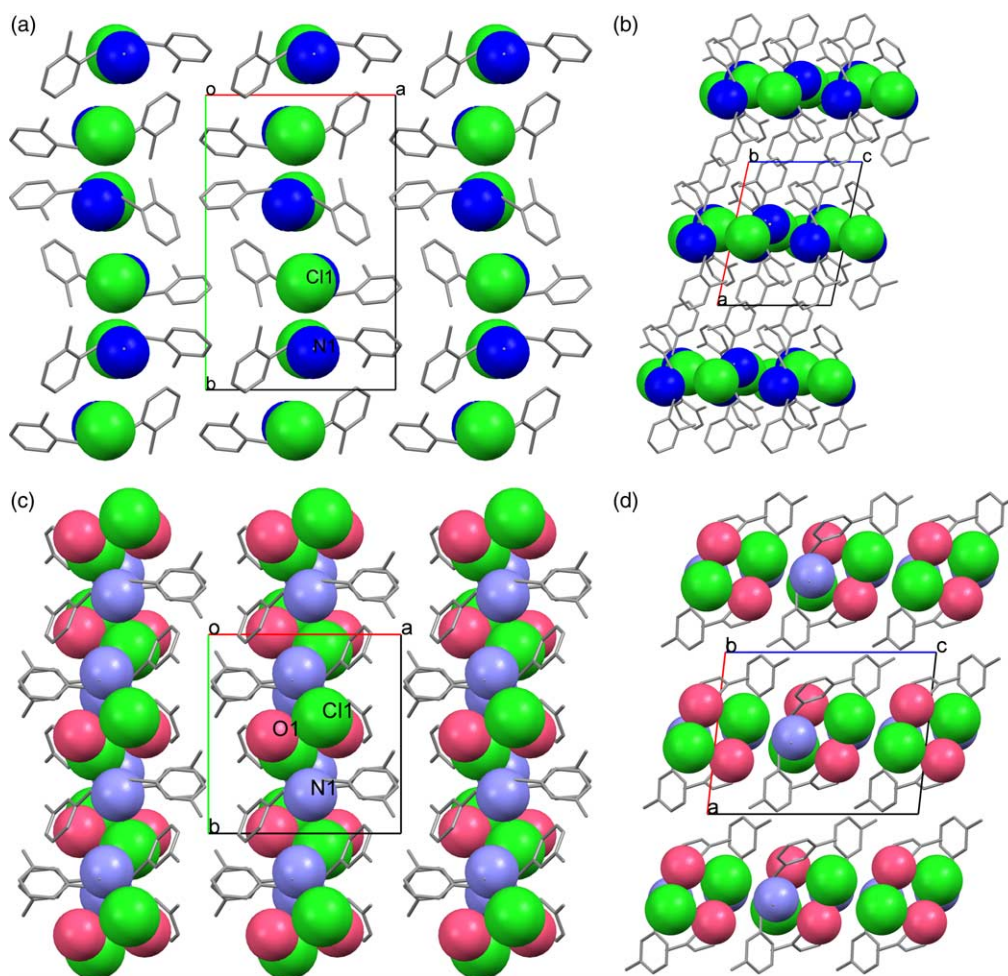

Fig. 4. The molecular packing of compounds **2** (a–b) and **3** (c–d). The cation and anion environments are enhanced by using Van der Waals space fills (N, smaller blue sphere, Cl, bigger green sphere). On (a) and (c) the structures are viewed along the crystallographic c-axis and similarly on (b) and (d) along the crystallographic b-axis; showing the chlorine–nitrogen and in case of **3** chlorine–nitrogen–oxygen layers (situated on bc-plane) along the crystallographic a-axis. The hydrogen atoms are omitted for clarity.

3. Results and discussion

3.1. Characterization in liquid and solid state

On the basis of ^1H and ^{13}C NMR methods, mass spectrometry and elemental analysis studies, all the compounds appeared pure and free of reaction solvents and other impurities. The exceptions are compounds **8** and **9**, which remained as sticky powders, despite several attempts to evaporate and dry the samples in vacuo. Based on the NMR measurements and elemental analysis, the products **8** and **9** contained small amounts of dichloromethane.

3.2. X-ray structure analysis

The crystallographic data of compounds 1–5 and 7 are shown in Table 1. The selected bond distances and angles are

gathered in Table 2. Compound **1** crystallized in monoclinic space group $C2/c$. This structure is not isomorphous with analogous bromide structure that crystallized in the monoclinic space group $P2_1/c$ [30]. In the case of the chloride structure, the chloride anion is disordered over two places (population parameters are about 0.5). The cation/anion pairs are interconnected by weak $Cl^-\cdots H–C$ bonds as the shortest bond distance is 2.68(1) Å for $H\cdots Cl^-$ (Fig. 1 [46]). In addition, the ion pairs are packed via intermolecular face to face π–π interactions between the phenyl groups as can be seen from Fig. 1(b).

The compounds **2**, **3** and **4** crystallized in the monoclinic space group $P2_1/c$ ($P2_1/n$). In cases of **2** and **3** the cation/anion pairs are interconnected by weak $Cl^-\cdots H–C$ bonds, the shortest bond distance being 2.63(1) Å for **2** and 2.64(1) Å for **3** (Figs. 2 and 3 [46]). Furthermore, in both cases the crystal packing is formed by aromatic interactions (especially edge to face interactions) between phenyl groups. The layer-like structure is observed for **2** and **3**. The nitrogen atoms, together with chloride anions form layers (situated on bc-plane) along
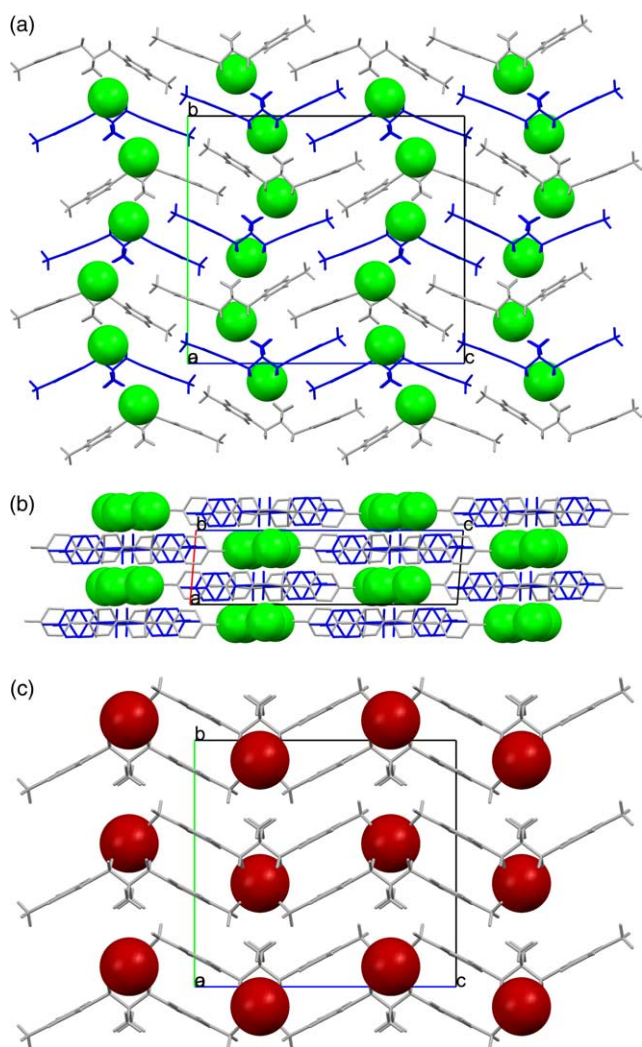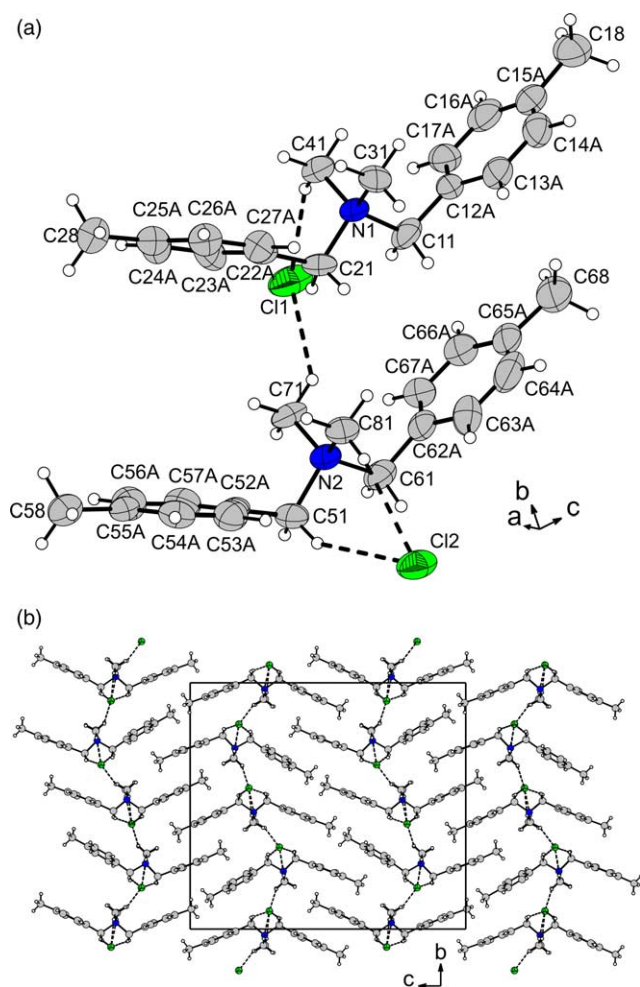

Fig. 5. (a) Ordering of the cations in the unit cell of compound **4** along the crystallographic *a*-axis and (b) along *b*-axis. Cations are colored based on their symmetry equivalence (dark blue, cation conformation 1, light grey, cation conformation 2). The chloride anions are enhanced by the Van der Waals space fills. (c) The ion-pair packing of non-isomorphous bromide analogue presented along *a*-axis [30]. The darker bromide anions are enhanced by the Van der Waals space fills.

Fig. 6. (a) The ion-pair ordering of compound **4**. (b) The packing of the ion-pairs with hydrogen bonding ($Cl^-\cdots H–C < 2.8$ Å) shown as dashed lines. The shortest cation/anion distances are C41···Cl1 3.59(2) Å, C71···Cl1 3.52(9) Å, C31···Cl2 3.49(6) Å and C81···Cl2 3.59(2) Å. The shortest distances from chloride anions to nitrogen atoms are about 3.88(3)–3.96(3) Å.

crystallographic *a*-axis and the aralkyl parts of the compounds stay between these nitrogen-chloride layers (Fig. 4 [47]). In the case of compound **3**, water molecule cocrystallized (molar ratio with main compound 1:1) into a structure, and consequently the hydrogen bonds between the water molecule and the chloride anion (bond distances $H \cdots Cl^-$ 2.29(4)–2.30(3) Å) have an effect on the crystal packing of **3**. The asymmetric unit of compound **4** contains two ion-pairs. The structure is not isomorphous with the analogous bromide that crystallizes in space group $C2/c$ [30]. Most likely the smaller chloride anion in the ion-pair causes a slight shift to the packing of the ion-pairs so that (Fig. 5(a) and (b)), compared to the bromide analogue (Fig. 5(c)), different packing mode is formed. Both cations appear in the W-conformation (Fig. 6 [46]) and are almost in the same conformation differing only slightly on the orientation of the other phenyl groups. The ion-pairs are packed in the way that both phenyl groups of the cation participate in the weak intermolecular face to face π–π interactions between the phenyl groups of the other ion-pairs forming phenyl group layers as can be seen from Fig. 6(b). Furthermore, the cation/anion pairs are interconnected by weak

$Cl^- \cdots H–C$ bonding, the shortest bond distance between chloride anions and hydrogen atoms being 2.67(2) Å.

Compound **5** crystallized in the triclinic space group *P*-1. The structure is isomorphous with the corresponding bromide described earlier [30]. The ion-pair ordering, hydrogen bonding ($H \cdots Cl^-$ < 2.8 Å) and the packing of **5** are presented in Fig. 7 [46]. The ion-pairs are interconnected by weak $Cl^- \cdots H–C$ bonding and the shortest $H \cdots Cl^-$ distance is 2.68(4) Å. Both phenyl rings of the cation are strongly turned towards each other forming continuous and alternating edge to face π–π interaction, in which every other connection between phenyl groups is intramolecular and the rest are intermolecular. The layer-like structure can also be observed for this structure.

Compound **7** crystallized in the orthorhombic space group *Pbca*, being also isomorphous with the analogous bromide structure [30]. The asymmetric unit of compound **7** consists of two ion-pairs whose cation conformations clearly differ from each other, as can be seen in Fig. 8. The weak $Cl^- \cdots H–C$ bonds affect the packing of **7** and the shortest $H \cdots Cl^-$ distance is 2.55(1) Å. The molecular packing is formed by both
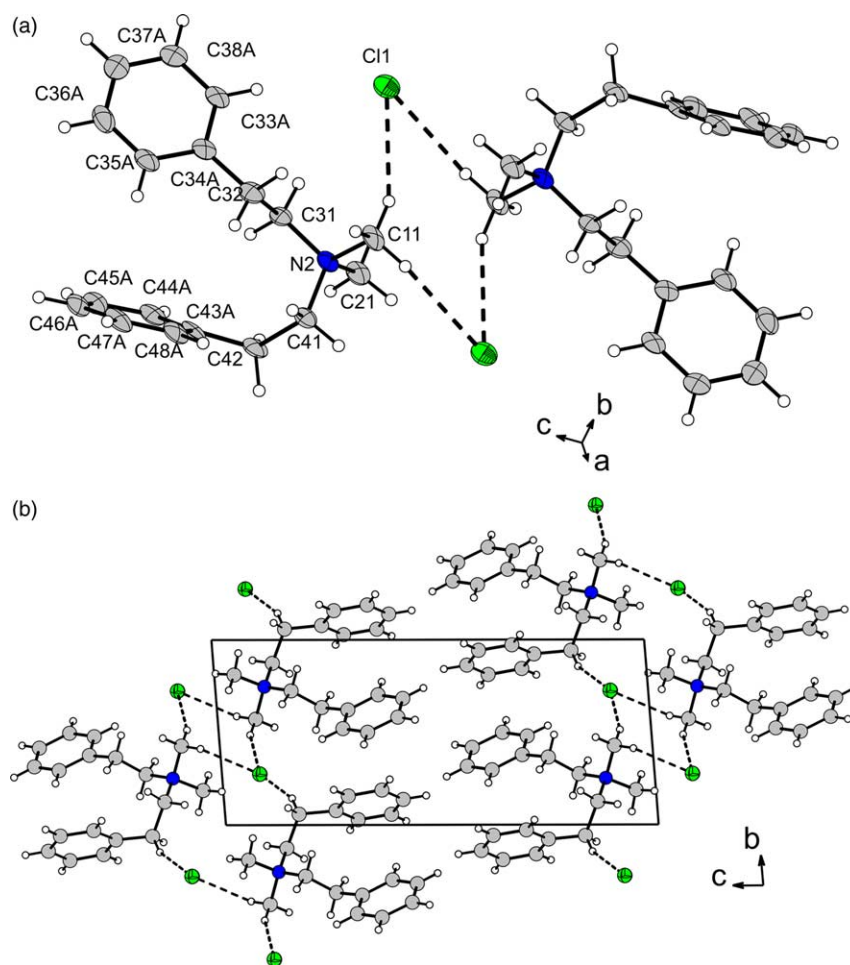

Fig. 7. (a) The ion-pair ordering of compound **5**. (b) Crystal packing viewed along the crystallographic *a*-axis with hydrogen bonding ($Cl^- \cdots H–C$ < 2.8 Å) shown as dashed lines. The shortest cation/anion distances are $C42 \cdots Cl1$ 3.63(5) Å and $C11 \cdots Cl1$ 3.66(6) Å. The distances from chloride anions to the adjacent nitrogen atoms are 4.16(4) and 4.23(6) Å.
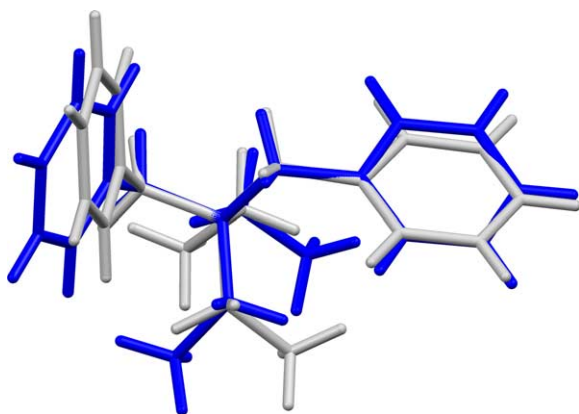
Fig. 8. Two different cation conformations found in the asymmetric unit of **7** (darker blue, cation conformation 1; lighter grey, cation conformation 2).

intramolecular CH···π interactions and intermolecular edge to face π–π interaction as can be seen from Fig. 9 [46].

3.3. Powder diffraction analysis

The experimental powder diffraction data of compounds **1**–**5** and **7** are presented in Fig. 10 together with the calculated diffraction data obtained from the single crystal structure parameters. In the case of compounds **2**, **4**, **5** and **7**, the

structural similarities between the bulk composition and single crystals can clearly be seen from Fig. 10.

In the case of compounds **1** and **3**, the calculated diffraction patterns were not congruent with experimental powder data, suggesting that compounds **1** and **3** can be crystallized in at least two polymorphic (or pseudo-polymorphic) forms so that the slowly-formed single crystals and the more quickly crystallized microcrystalline powder can actually end up as different polymorphs. The solid state NMR spectra of compounds **1** and **3** were measured to confirm the number of polymorphs in the bulk composition. The spectra are presented in Fig. 11. The ^{13}C CP MAS solid state NMR spectra showed that the compound **3** has two different polymorphs in its bulk composition which still differ from the solved single crystal structure. Therefore, three polymorphs of **3** can be found; one at low temperature (-100 °C) and two at room temperature. In the case of compound **1**, one polymorph was seen in the ^{13}C CP/MAS solid state NMR spectrum meaning that two polymorphs were found overall; one at low temperature and one at room temperature.

3.4. Thermal properties

The TG and DTA curves for compounds **1**–**9** are presented in Fig. 12. The results of DSC measurements are summarized
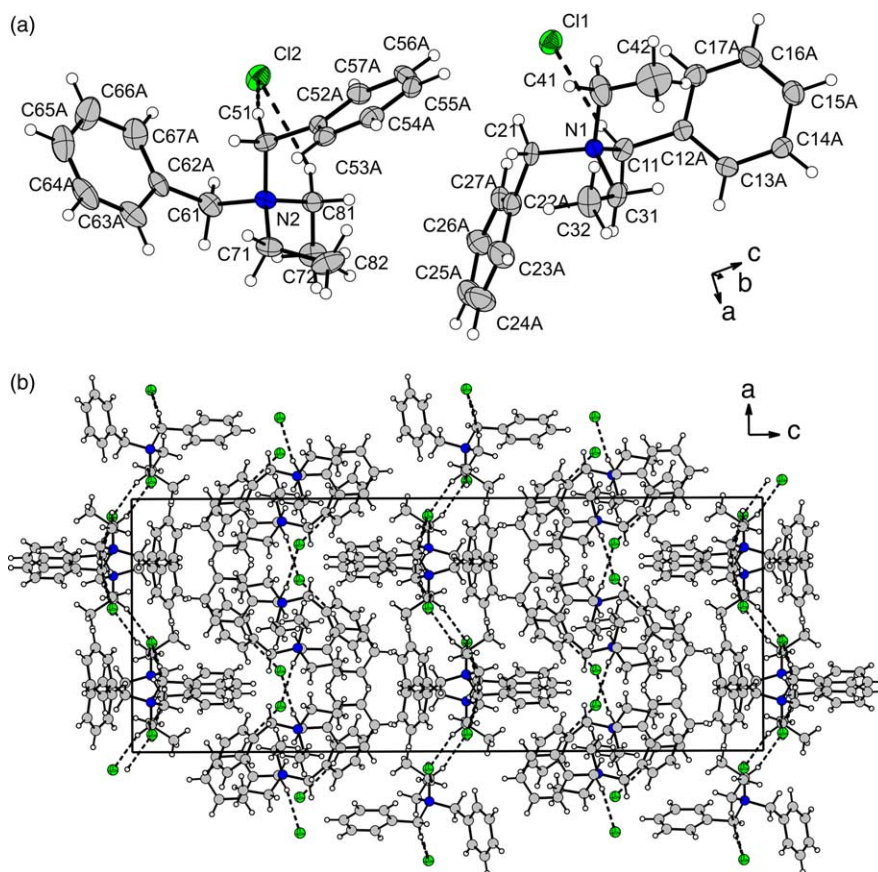

Fig. 9. (a) The ion-pair ordering of compound **7** (b) packing of **7** along the crystallographic *b*-axis with hydrogen bonding (Cl$^-$···H–C<2.8 Å) shown as dashed lines. The shortest cation/anion distances are C71···Cl2 3.49(1) Å, C11···Cl1 3.50(1) Å and C13A···Cl1 3.57(1) Å. The distances of the chlorides anion to the nearest nitrogen atoms are 4.08(1) Å and 3.92(1) Å.
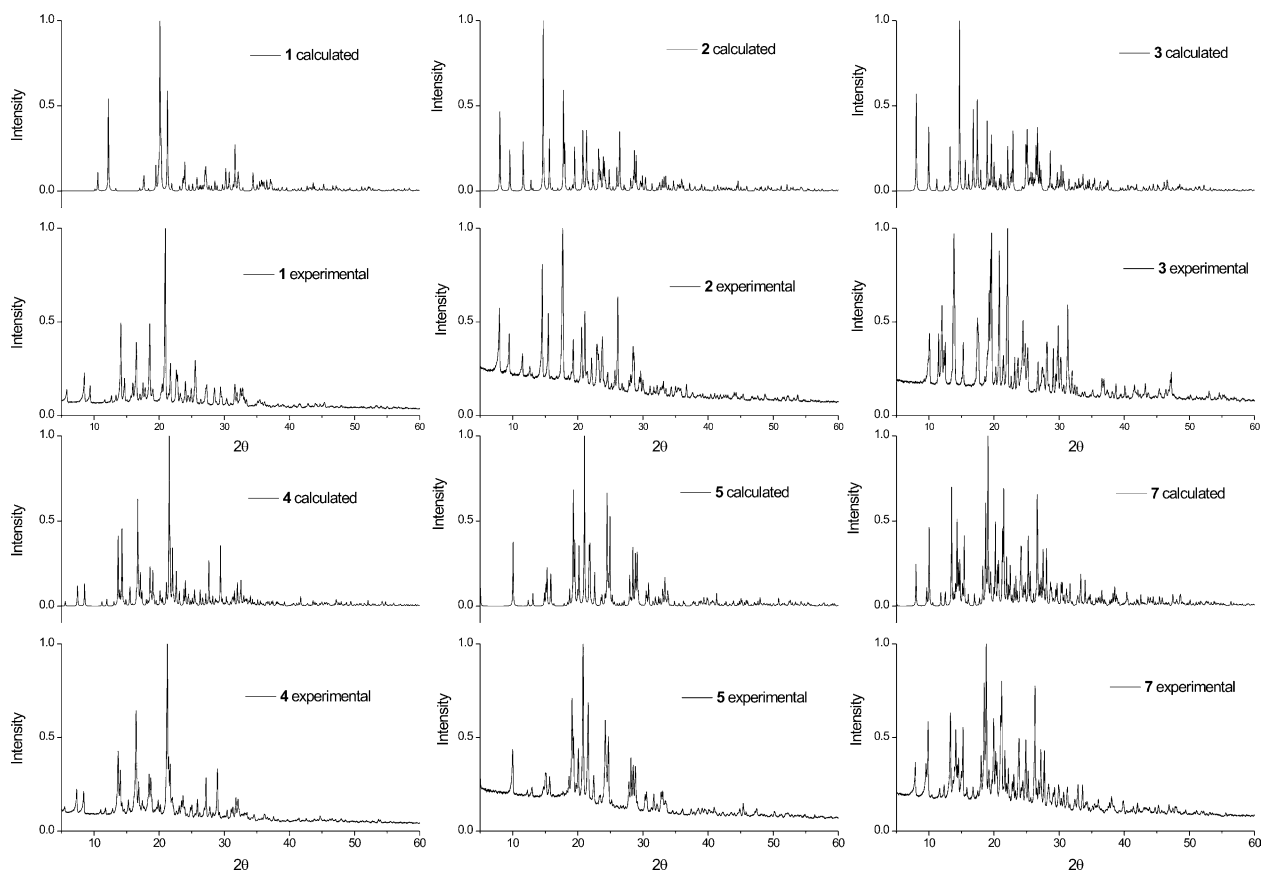
Fig. 10. Experimental powder data of **1**–**5** and **7** compared with calculated data which were obtained from the single crystal structure parameters.

in Table 3. The transition peaks of DSC curves were taken from peak onsets. Furthermore, in the case of compound **5** the observed melting point was confirmed with melting point apparatus.

Generally, all the compounds decomposed without identifiable cleavages. In the case of compounds **1**, **2**, **4** and **7**, no phase-transitions were observed using DTA or DSC measurements before decomposition which started at temperatures 160, 170, 185 and 140 °C, respectively. The compounds **6** and **8**, **9** remained as sticky powders or viscous oil, even though several attempts were made to crystallize and dry them. Consequently, only the glass transitions were obtained using DSC at temperatures −20.4, −23.2 and 8.1 °C, respectively. No other events were observed for compounds **6**, **8** and **9** before decomposition, which started at temperatures 155, 85 and 130 °C, respectively. In the case of compound **3**, the melting point was observed just before decomposition at 150 °C, as can be seen from Fig. 12 and from the DSC measurement (Table 3). Compound **5** was the only clearly crystalline compound showing the sharp melting peak (138.0 °C) and consequently, a liquid range of about 30 °C was seen before the decomposition which started at 170 °C. The observed decomposition ranges of synthesized quaternary dialkyldiaralkylammonium chlorides (for compounds **1**, **4**, **5**–**7** and **9**) were observed to be quite similar to those that were obtained for corresponding bromides, as can be seen from Table 3.
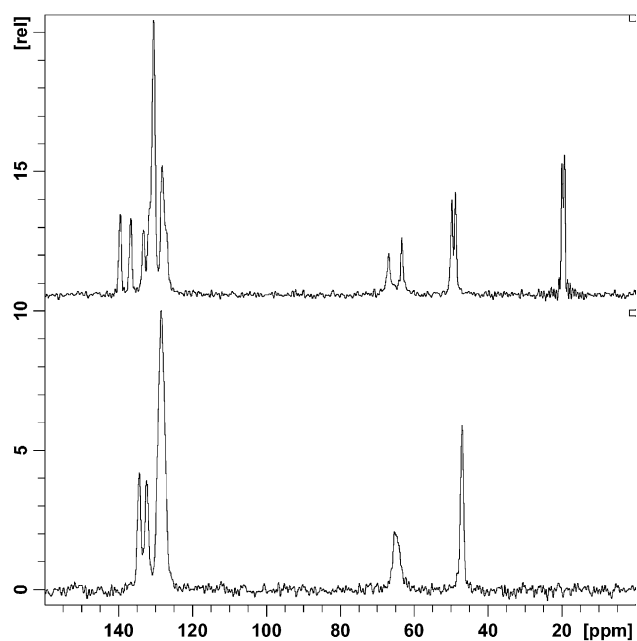

Fig. 11. The solid state NMR spectra of compound **1** (lower) and **3** (upper). In the case of **3** two polymorphs can be seen in the spectrum as the assigned carbon signals of the second polymorph are slightly shifted compared to the signals of the first polymorph.

Table 1
Crystallographic data for compounds 1–5 and 7

Compound	1	2	3	4	5	7
Formula	C$_{16}$H$_{20}$NCl	C$_{18}$H$_{24}$NCl	C$_{18}$H$_{24}$NCl·H$_2$O	C$_{18}$H$_{24}$NCl	C$_{18}$H$_{24}$NCl	C$_{18}$H$_{24}$NCl
M_r (g mol^{-1})	261.78	289.83	307.85	579.66	289.83	579.66
Crystal system	Monoclinic	Monoclinic	Monoclinic	Monoclinic	Triclinic	Orthorhombic
Space group	C2/c	P2$_1$/c	P2$_1$/c	P2$_1$/n	P-1	Pbca
a [Å]	18.537(4)	11.260(9)	11.042(2)	6.584(5)	5.803(2)	14.135(4)
b [Å]	10.085(2)	17.087(5)	11.352(2)	21.207(9)	7.571(2)	12.765(5)
c [Å]	17.780(4)	8.713(2)	14.293(2)	23.761(5)	17.654(3)	35.215(5)
α [°]	90	90	90	90	85.61(3)	90
β [°]	109.969(16)	102.32(7)	96.347(6)	94.70(7)	87.115(17)	90
γ [°]	90	90	90	90	89.82(3)	90
V [Å^3]	3124.1(10)	1637.7(14)	1780.5(3)	3307(3)	772.4(3)	6354(3)
Z	8	4	4	8	2	16
ρ_{calcd} (g cm^{-3})	1.113	1.175	1.148	1.164	1.246	1.212
μ (mm^{-1})	0.229	0.225	0.214	0.222	0.238	0.232
T (K)	173(2)	173(2)	173(2)	173(2)	173(2)	173(2)
F(000)	1120	624	664	1248	312	2496
Crystal size (mm)	0.30×0.25×0.15	0.30×0.30×0.20	0.30×0.30×0.10	0.10×0.10×0.10	0.40×0.20×0.10	0.30×0.15×0.05
θ Range (°)	3.07–27.50	3.02–25.00	3.05–25.00	3.01–25.10	3.42–27.50	3.11-25.00
Reflections collected	12451	9614	15857	38382	12775	29963
Independent reflections	3355	2870	3132	5813	3528	5521
Data/Restraints/Parameters	3355/0/174	2870/0/182	3132/3/197	5813/0/362	3528/0/181	5521/0/362
GooF	1.068	1.021	1.029	1.059	1.029	1.020
R(int)	0.0505	0.0493	0.0519	0.2109	0.0987	0.1612
Final R indices [$I > 2\sigma(I)$], R1/wR2	0.0948/0.2808	0.0518/0.1257	0.0632/0.1767	0.1033/0.2514	0.0823/0.1901	0.0696/0.1250
R indices (all data), R1/wR2	0.1646/0.3286	0.0941/0.1472	0.1134/0.2057	0.2456/0.3329	0.1537/0.2214	0.1900/0.1572
Largest diff.peak/hole [e Å^{-3}]	1.147/−0.282	0.706/−0.319	0.910/−0.377	0.361/−0.402	0.598/−0.782	0.839/−0.284

4. Conclusions

Nine aromatic R$_2$R$_2'$N$^+$Cl$^-$ quaternary dialkyldiaralkylammonium chlorides were synthesized by a method in which dimethylformamide or diethylformamide was treated with non-substituted or substituted aralkyl halide in the presence of sodium carbonate. Six of the compounds precipitated as microcrystalline powder (1–5 and 7) and three of the compounds remained as viscous oil or sticky powder (6, 8 and 9). The crystal structures of all crystalline compound (1–5 and 7) were determined using X-ray single crystal diffraction after recrystallization from a MeOH/EtOAc solution. Two of the crystalline compounds were isomorphous with corresponding bromide salts (5 and 7) which were reported earlier [30] and two of the chlorides (1 and 4) crystallized in a different space group than their analogous bromides. The compounds 2 and 3 have not been synthesized as bromides. The powder diffraction data were measured to investigate the structural similarities with the microcrystalline bulk composition and in four of the cases (compounds 2, 4, 5 and 7) the calculated diffraction

Table 2
Selected bond lengths (Å) and bond angles (°) of compounds 1–5 and 7

| Compound	1	2	3	4	5	7
N(1)–C(11)	1.523(5)	1.532(3)	1.529(4)	1.518(7)	1.515(4)	1.528(4)
N(1)–C(21)	1.530(5)	1.525(3)	1.531(4)	1.528(7)	1.515(4)	1.515(4)
N(1)–C(31)	1.486(5)	1.484(4)	1.492(4)	1.503(8)	1.514(4)	1.494(5)
N(1)–C(41)	1.491(5)	1.488(4)	1.484(4)	1.473(8)	1.497(4)	1.531(5)
C(11)–N(1)–C(21)	108.9(3)	105.7(2)	106.4(2)	104.3(4)	107.6(3)	107.3(3)
C(11)–N(1)–C(31)	110.9(3)	110.2(2)	110.5(2)	110.3(5)	111.0(3)	108.6(3)
C(11)–N(1)–C(41)	110.2(3)	110.7(2)	110.5(2)	112.3(5)	107.2(3)	111.1(3)
C(21)–N(1)–C(31)	110.6(3)	110.8(2)	109.7(2)	109.1(5)	106.7(3)	112.7(3)
C(21)–N(1)–C(41)	107.5(3)	109.6(2)	110.5(3)	111.5(5)	109.7(3)	104.3(3)
C(31)–N(1)–C(41)	108.8(3)	109.9(2)	109.3(3)	109.2(5)	114.5(2)	112.7(3)
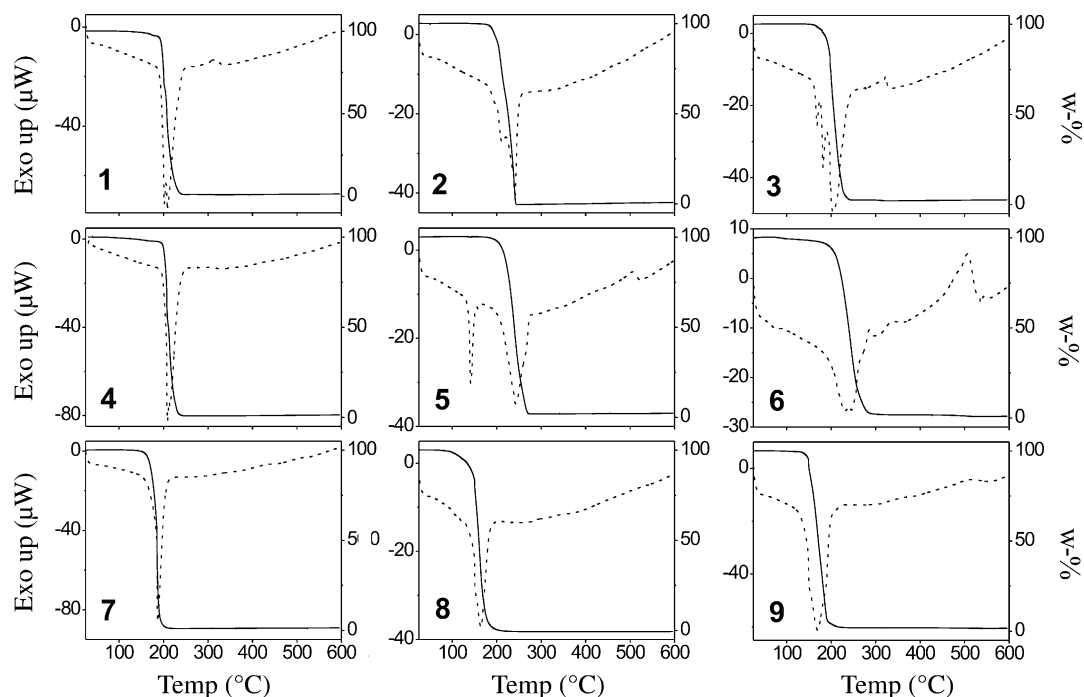
Fig. 12. TG (solid line) and DTA (dashed line) curves for compounds **1**–**9**. The exothermic events are pointing up in the DTA curves.

Table 3
Phase-transition (DSC onsets) and melting points (DSC onsets) temperatures, enthalpy changes and decomposition ranges (the starting value were taken from the initial mass loss of the decomposition) for compounds **1**–**9**

Compound	Glass transition temperature T_g and ΔC_p (°C, (J g^{-1} °C^{-1}))	T_m and enthalpy change (°C, (J g^{-1}))	Decomposition range (°C)	Decomposition range of analogous bromide (°C) [30]
1			160–250	165–245
2			170–250	
3		149.1 (24.49)	150–250	
4			185–245	190–270
5		138.0 (118.2)	170–280	190–300
6	−20.4 (0.593)		155–300	180–300
7			140–215	165–230
8	−23.2 (0.421)		85–225	
9	8.1 (0.433)		130–235	135–300

patterns were congruent with the experimental powder diffraction pattern, confirming the structural similarity between the low and room temperature structures. For compounds **1** and **3**, the powder diffraction data and the ^{13}C CP/MAS NMR spectra, together with the single crystal structures, showed that compound **1** can be crystallized in at least two polymorphic forms and compound **3** in at least three polymorphic forms.

The synthesized chlorides are less suitable for ionic liquid applications compared to the corresponding bromides presented earlier [30], because only two of the nine synthesized chlorides showed a melting point. Furthermore, compound **3** melted just before decomposition, therefore no liquid range existed. In the case of compound **5**, a liquid range of 30 °C was observed before the decomposition (starting at 170 °C), but the melting point of 138.0 °C is generally too high for most ionic liquid applications. However, good thermal stability of these

synthesized chlorides enables their potential use as phase-transfer catalysts and electrolytes, for example.

5. Supporting information available

CCDC 261836-261841 contains the supplementary crystallographic data for this paper. These data can be obtained free of charge from The Cambridge Crystallographic Data Centre via www.ccdc.cam.ac.uk/data_request/cif.

References

[1] S. Haas, H. Hoffmann, Prog. Polym. Sci. 101 (1996) 131–134.

[2] F. Menger, J. Keiper, Angew. Chem. Int. Ed. 39 (2000) 1907–1920.

[3] M. In, V. Bec, O. Aguerre-Chariol, R. Zana, Langmuir 16 (2000) 141–148.

[4] B. Bales, R. Zana, J. Phys. Chem. B 106 (2002) 1926–1939.

[5] A. Wiacek, E. Chibowski, K. Wilk, Colloids Surf., A 193 (2001) 51–60.

[6] X. Li, S. Goh, Y. Lai, S-M. Deng, J. Appl. Polym. Sci. 73 (1999) 2771–2777.

[7] T. Ooi, Y. Uematsu, M. Kameda, K. Maruoka, Angew. Chem. Int. Ed. 41 (2002) 1551–1554.

[8] J. Shimizu, T. Nagami, H. Mikawa, Solid Sate Ionics 14 (1984) 153–157.

[9] K. Cathro, K. Cedzynska, D. Constable, P. Hoobin, J. Power Sources 18 (4) (1986) 349–370.

[10] P. Hoobin, K. Cathro, J. Niere, J. Appl. Electrochem. 19 (6) (1989) 943–945.

[11] K. Cedzynska, Electrochim. Acta 40 (8) (1995) 971–976.

[12] J.B. Welch, Eur. Pat. Appl. (1984).

[13] M. Nakayama, S. Konishi, H. Tagashira, K. Ogura, Langmuir 21 (2005) 354–359.

[14] G. Kano, M. Aoki, T. Endo, G. Shibamoto, Jpn. Kokai Tokkyo Koho (2003).

[15] K. Murayama, A. Katsuyuki, Chem. Commun. 5 (1998) 607–608.

[16] C. Schalley, T. Martin, U. Obst, J. Rebek, J. Am. Chem. Soc. 121 (1999) 2133–2138.

[17] A. Shivanyuk, J. Rebek, Chem. Commun. 22 (2001) 2374–2375.

[18] H. Mansikkamäki, M. Nissinen, K. Rissanen, Chem. Commun. 17 (2002) 1902–1903.

[19] H. Mansikkamäki, M. Nissinen, C. Schalley, K. Rissanen, New J. Chem. 27 (2003) 88–97.

[20] H. Mansikkamäki, M. Nissinen, K. Rissanen, Angew. Chem. Int. Ed. 43 (2004) 1243–1246.

[21] J.A. Creighton, K.M. Thomas, J. Chem. Soc., Dalton Trans.: Inorg. Chem. 3 (1972) 403–410; J.A. Creighton, K.M. Thomas, J. Chem. Soc., Dalton Trans.: Inorg. Chem. 20 (1972) 2254–2257.

[22] R.D. Willett, J.A. Haugen, J. Lebsack, J. Morrey, Inorg. Chem. 13 (1974) 2510–2513.

[23] A. Uehara, A. Iimura, K. Shimizu, S. Morita, A. Yoshifuji, R. Tsuchiya, H. Imai, Y. Uemori, S. Nakagawa, E. Kyuno, Thermochim. Acta 77 (1984) 299–309.

[24] A. Ghosh, G. De, N. Ray Chaudhuri, Thermochim. Acta 108 (1986) 97–103.

[25] H. Place, R.D. Willet, Acta Crystallogr. C 44 (1988) 34–38.

[26] R.D. Willett, M. Wei, J. Phys. Chem. Solids 61 (2000) 2025–2028.

[27] R. Nicholson, Y. Fujii, X. Chen, R. Willett, J. Phys. Chem. Solids 62 (2001) 933–940.

[28] R.D. Willett, C. Galeriu, C.P. Landee, M.M. Turnbull, B. Twamley, Inorg. Chem. 43 (2004) 3804–3811.

[29] J. Ropponen, M. Lahtinen, S. Busi, M. Nissinen, E. Kolehmainen, K. Rissanen, New J. Chem. 28 (2004) 1426–1430.

[30] S. Busi, M. Lahtinen, J. Ropponen, J. Valkonen, K. Rissanen, J. Solid State Chem. 177 (2004) 3757–3767.

[31] S. Busi, M. Lahtinen, H. Mansikkamäki, J. Valkonen, K. Rissanen, J. Solid State Chem. 178 (2005) 1722–1737.

[32] M.S. Kharasch, G.N. Williams, W. Nudenberg, J. Org. Chem. 20 (1955) 937–952.

[33] M. Makosza, B. Serafin, Roczniki Chemii 39 (1965) 1223–1230.

[34] U. Anthoni, C. Christophersen, P.H. Nielsen, Synth. Commun. 31 (2001) 2223–2229.

[35] H. Guemmour, F. Carriere, A. Benaboura, Polym. Bull. 46 (2001) 1–6.

[36] K.B.B. Pathak, H.K. Das, J. Indian Chem. Soc. 75 (1998) 180.

[37] D. Christensen, K.A. Joergensen, J. Org. Chem. 54 (1989) 126–131.

[38] W.J. Criddle, J. Thomas, J. Anal. Appl. Pyrolysis 2 (1981) 361–368.

[39] F.J. Lombardi, J.P. Reeves, H.R. Kaback, J. Biol. Chem. 248 (1973) 3551–3565.

[40] G.P. Schiemenz, Tetrahedron 29 (1973) 741–745.

[41] A.R. Lepley, A.G. Giumanini, J. Org. Chem. 32 (1967) 1706–1713.

[42] A.J.M. Duisenberg, L.M.J. Kroon-Batenburg, A.M.M. Schreurs, J. Appl. Crystallogr. (2003) 220–229.

[43] A. Altomare, G. Cascarano, C. Giacovazzo, A. Guagliardi, SIR92: a program for crystal structure solution, J. Appl. Crystallogr. 26 (1993) 343–350.

[44] A. Altomare, M. Burla, M. Camalli, G. Cascarano, C. Giacovazzo, A. Guagliardi, A. Moliterni, G. Polidori, R. Spagna, SIR97: a program for crystal structure solution, J. Appl. Crystallogr. 32 (1999) 115–119.

[45] Sheldrick G.M., SHELXL−97 — A Program for Crystal Structure Refinement, University of Gottingen, Germany, 1997.

[46] Branderburg K., DIAMOND, v 3.0b, Crystal Impact GbR Bonn, Germany, 2005.

[47] I.J. Bruno, J.C. Cole, P.R. Edginton, M.K. Kessler, C.F. Macrae, P. McCabe, J. Pearson, R. Taylor, MERCURY 1.4, Acta Crystallogr. B58 (2002) 389–397.